Generation and Characterization of IDH1^{R132H} and IDH2^{R140Q} *In Vitro* Models for Drug Discovery

Diana Douglas [1], Lysa-Anne Volpe [2], Luping Chen [2], Metewo Selase Enuameh [1], Fang Tian [2], and Weiguo Shu [1]

[1]ATCC Cell Systems, Gaithersburg, MD 20877, USA; [2]ATCC, Manassas, VA 20110, USA

AACR Abstract # 3106

Abstract

Isocitrate dehydrogenase (IDH) is a metabolic enzyme that converts isocitrate to α-ketoglutarate (α-KG). Mutations in this enzyme have been linked to human cancers such as glioma and acute myeloid leukemia (AML)[1]. While there are three isoforms of IDH, mutations that lead to cancer have only been identified in IDH1 and IDH2, which result in simultaneous loss of normal catalytic activity, the production of α-KG, and the gain of a new function—the production of 2-hydroxyglutarate D-2HG[2]. D-2HG is structurally similar to α-KG and acts as an α-KG antagonist to competitively inhibit multiple α-KG-dependent dioxygenases, including lysine histone demethylases (KDM) and DNA hydroxylases (TET), causing widespread changes in histone and DNA methylation and potentially promoting tumorigenesis[3]. A number of studies from the mutant IDH inhibitors indicate that IDH is a valid target for a new class of cancer therapeutics[4-6].

The most prominent IDH1 mutation takes place at residue R132H and plays a role in the development of gliomas, while the majority of IDH2 mutations take place at residue R140Q, which is linked to AML[7]. Given the prevalence of these mutations, we sought to use CRISPR/Cas9 gene-editing technology to create two *in vitro* disease models that harbor either the IDH1 or IDH2 mutations. An IDH1^{R132H} G >A mutation was introduced in the malignant glioblastoma U-87 MG (ATCC® HTB-14™) cell line, and an IDH2^{R140Q} G>A mutation was introduced in the TF-1 (ATCC® CRL-2003™) erythroblast cell line that was derived from an AML patient. To validate that the isogenic IDH mutations confer gain-of-function *in vitro*, we tested the intracellular and extracellular levels of D-2HG. Bio-functional evaluation data indicated that the IDH1^{R132H} mutant U-87 MG Isogenic Cell Line (ATCC® HTB-14IG™) showed an increase in cellular D-2HG and elevated level of histone methylation. In the IDH2^{R140Q} mutant TF-1 Isogenic Cell Line (ATCC® CRL-2003IG™), an increase in cellular D-2HG was also observed. In response to IDH2-specific inhibitors, AG-221[4] and AGI-6780[5], we demonstrated that IDH2^{R140Q} TF-1 cells exhibited decreases in both cellular D-2HG and histone methylation levels. Taken together, these data demonstrate that isogenic *in vitro* models are valuable tools for elucidating mechanisms involved in cancer-associated tumorigenesis and use in screening anti-cancer compounds for drug discovery.

I. Background Information

Mechanisms of Mutant IDH1 and IDH2 in Tumorigenesis

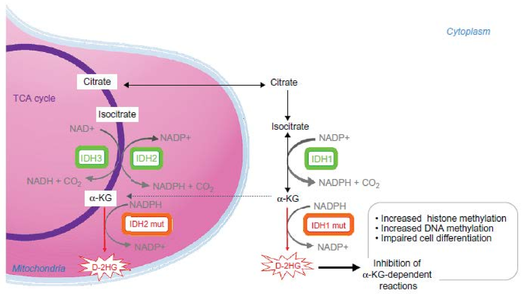

Figure 1. Enzymatic activities of wild-type (WT) and mutated IDH enzymes[7]. WT IDH enzymes catalyze the production of α-KG, and mutant IDH proteins gain neomorphic enzymatic activity, converting α-KG to D-2HG. D-2HG inhibits α-KG–dependent dioxygenases. Excess D-2HG is associated with increased histone and DNA methylation, altering cancer cell differentiation.
This diagram was adapted from Mondesir J, *et al. J Blood Med* 7: 171–180, 2016.

II. Generation of IDH1^{R132H} and IDH2^{R140Q} Knock-In Alleles

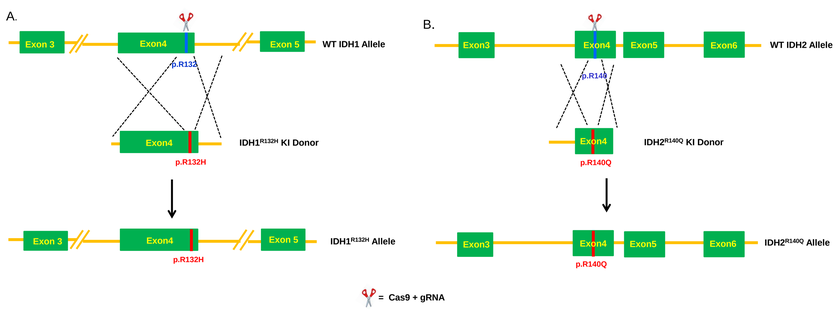

Figure 2. Gene-editing knock-in strategy for the generation of the IDH1^{R132H} allele in U-87 MG cells (A) and IDH2^{R140Q} allele in TF-1 cells (B). U-87 MG and TF-1 parental cells were transfected with respective gRNA and knock-in donor, along with the Cas9 expressing plasmid. Transfected cells were then subjected to transient antibiotic selection and the surviving pooled cells were used for single cell sorting. The expanded single cell clones were then subjected to genotyping to identify clones harboring the desired knock-in mutations.

III. Identification of IDH1^{R132H} and IDH2^{R140Q} Alleles in the Genome

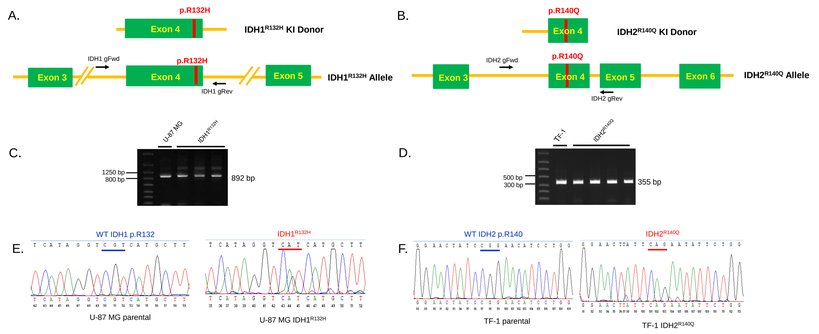

Figure 3. Identification of the IDH1^{R132H} knock-in allele in U-87 MG cells and IDH2^{R140Q} knock-in allele in TF-1 cells. Genomic DNA was extracted from U-87 MG and TF-1 parental cell expanded single clones and was subjected to junction PCR and Sanger sequencing analysis. (A, B) IDH1 and IDH2 junction PCR primers and their positions are displayed in the diagram. (C, D) Junction PCR amplicons from parental U-87 MG cells, potential IDH1^{R132H} clones, parental TF-1 cells, and potential IDH2^{R140Q} clones were separated on agarose gels. (E) Amplicon Sanger sequencing data for parental U-87 MG cells and IDH1^{R132H} knock-in cells showed the successful knock-in of p.R132H (c.395G>A). (F) Sanger sequencing data for parental TF-1 cells and IDH2^{R140Q} knock-in cells indicated the successful knock-in of p.R140Q (c.419G>A).

IV. Confirmation of IDH1^{R132H} and IDH2^{R140Q} Alleles in RNA Transcripts

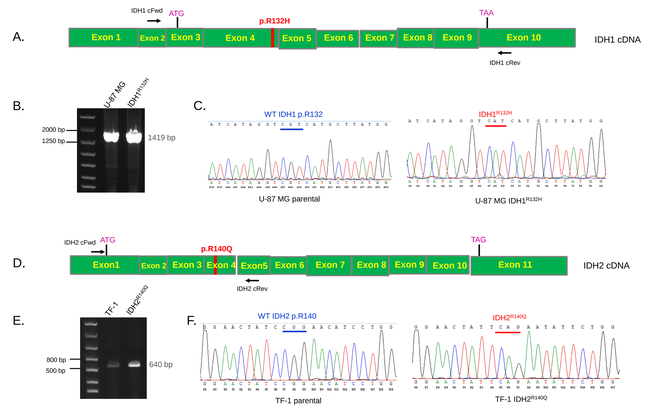

Figure 4. Confirmation of the IDH1^{R132H} knock-in allele in U-87 MG cells and the IDH2^{R140Q} knock-in allele in TF-1 cells. (A,D) Diagram of IDH1 and IDH2 cDNA displays the PCR primers. (B, E) PCR amplicons from the cDNA of parental U-87 cells, IDH1^{R132H} U-87 MG cells, parental TF-1 cells, and IDH2^{R140Q} TF-1 cells were separated on agarose gels. (C) cDNA amplicon Sanger sequencing data for parental U-87 MG cells and IDH1^{R132H} knock-in cells confirmed the transcription of IDH1^{R132H} (c.395G>A) knock-in mutation in gene-edited cells. (F) cDNA amplicon Sanger sequencing data for parental TF-1 cells and IDH2^{R140Q} knock-in cells confirmed the transcription of IDH2^{R140Q} (c.419G>A) knock-in mutation in gene-edited cells.

V. Morphology of IDH1^{R132H} U-87 MG and IDH2^{R140Q} TF-1 Cells

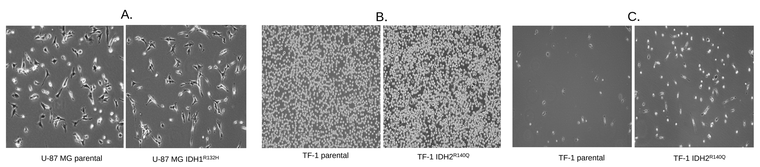

Figure 5. Morphology of IDH1^{R132H} mutant U-87 MG cells and IDH2^{R140Q} mutant TF-1 cells. (A) IDH1^{R132H} U-87 MG cells displayed morphology similar to parental U-87 MG cells. (B) Suspension culture of parental TF-1 cells and IDH2^{R140Q} TF-1 cells in complete culture media. (C) After removing the suspension cells, a larger population of IDH2^{R140Q} TF-1 cells attached to the tissue culture plate and exhibited spindle-like morphology (undifferentiated mesenchymal-like cells) when compared to parental TF-1 cells.

VI. Growth Kinetics of IDH1^{R132H} and IDH2^{R140Q} Mutant Cells

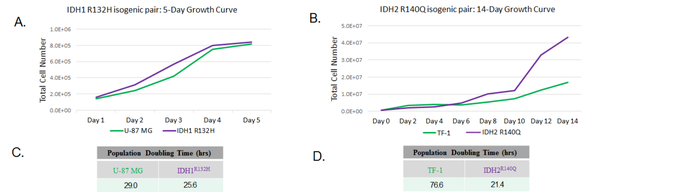

Figure 6. Growth curve of IDH1^{R132H} U-87 MG cells and IDH2^{R140Q} TF-1 cells. (A) Growth of parental U-87 MG cells (green line) and IDH1^{R132H} U-87 MG cells (purple line) was measured over 5 days, and the calculated population doubling time for parental U-87 MG cells and IDH1^{R132H} U-87 MG cells is shown in (C). (B) parental TF-1 cells (green line) and IDH2^{R140Q} TF-1 cells (purple line) were cultured in granulocyte-macrophage colony-stimulating factor (GM-CSF)–free medium; growth was measured over 14 days. (D) Population doubling time for parental TF-1 cells and IDH2^{R140Q} TF-1 cells. While parental TF1 cells were GM-CSF–dependent, IDH2^{R140Q} TF-1 cells exhibited GM-CSF–independent proliferation[5].

VII. Phenotypic Characterization of IDH1^{R132H} U-87 MG Cells

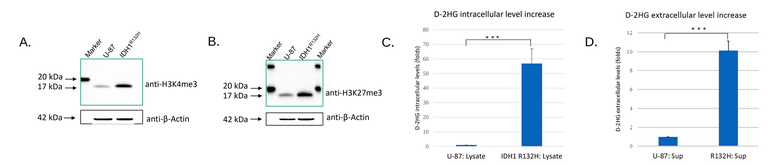

Figure 7. Increased histone methylation and D-2HG accumulation in IDH1^{R132H} U-87 MG cells. (A, B) Western blot analysis of parental U-87 MG cells and IDH1^{R132H} U-87 MG cells using H3K4me3 and H3K27me3 antibodies showed histone hyper-methylation in IDH1^{R132H} U-87 MG cells. β-Actin was used as a loading control. (C) The intracellular D-2HG level was measured in parental U-87 MG cells and IDH1^{R132H} U-87 MG cells via the PicoProbe™ (BioVision) assay. (D) The extracellular D-2HG level was measured in parental U-87 MG and IDH1^{R132H} U-87 MG cells via the PicoProbe™ assay. Elevated D-2HG levels were detected in IDH1^{R132H} mutant cells (n=3, Student's t-test, ***p<0.001).

VIII. Phenotypic Characterization of IDH2^{R140Q} TF-1 Cells

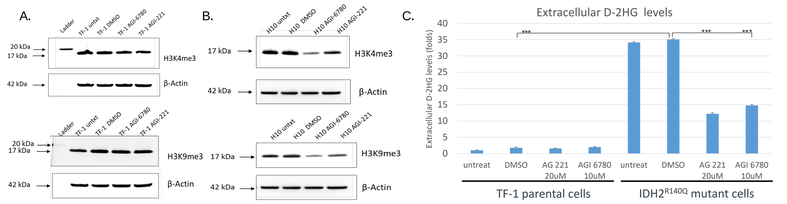

Figure 8. Decreased histone methylation and D-2HG accumulation in IDH2^{R140Q} cells in response to IDH2 specific inhibitors. Western blot analysis of (A) TF-1 parental and (B) IDH2^{R140Q} TF-1 cells using H3K4me3 and H3K9me3 antibodies was performed. (B) In response to treatment with IDH2^{R140Q}-specific inhibitors, AGI-6780 and AGI-221, IDH2^{R140Q} TF-1 cells exhibited decreased histone methylation levels, but (A) TF-1 parental cells did not show a histone methylation change in response to the same drug treatment. β-Actin was used as a loading control for both (A) and (B). (C) Untreated and DMSO treated IDH2^{R140Q} TF-1 cells showed increased extracellular D- 2HG level compared to TF-1 parental cells under the same condition. IDH2^{R140Q} TF-1 cells were able to respond to treatment with IDH2^{R140Q}-specific inhibitors AGI-6780 and AGI-221, and exhibited a decrease in extracellular D-2HG levels as measured by PicoProbe™ assay (n=3, Student's t-test, ***p<0.001).

Summary

- We have successfully generated IDH1^{R132H} U-87 MG and IDH2^{R140Q} TF-1 cell lines via CRISPR/Cas9 gene editing.
- The IDH1^{R132H} U-87 MG cell line showed morphology similar to the parental cell line. IDH1^{R132H} U-87 MG cells exhibited increased intracellular and extracellular D-2HG levels, leading to histone hyper-methylation.
- A population of IDH2^{R140Q} TF-1 cells attached to the tissue culture plate and displayed spindle-like morphology, which is a characteristic of undifferentiated mesenchymal cells. IDH2^{R140Q} TF-1 cells exhibited increased cellular D-2HG level. More importantly, IDH2^{R140Q} TF-1 cells were able to respond to treatment with the IDH2^{R140Q}-specific inhibitors AGI-6780 and AGI-221, and showed a reduction in cellular D-2HG accumulation, leading to the decrease of histone methylation.
- IDH1^{R132H} U-87 MG and IDH2^{R140Q} TF-1 cell lines are valuable tools for studying cancer biology and for use in screening anti-cancer compounds for drug discovery.

References

1. Yang H, *et al.* IDH1 and IDH2 mutations in tumorigenesis: mechanistic insights and clinical perspectives. Clin Cancer Res 18(20): 5562-5571, 2012. PubMed: 23071358
2. Luchman HA, *et al. An in vivo* patient-derived model of endogenous IDH1-mutant glioma. Neuro Oncol 14(2):184–191, 2012. PubMed: 22166263
3. Han CH, *et al.* Isocitrate dehydrogenase mutation as a therapeutic target in gliomas. Chin Clin Oncol 6(3):33, 2017. PubMed: 28705010
4. YenK, *et al.* AG-221, a first-in-class therapy targeting acute myeloid leukemia harboring oncogenic IDH2 mutations. Cancer Discov 7(5):478-493, 2017. PubMed: 28193778
5. Wang F, *et al.* Targeted inhibition of mutant IDH2 in leukemia cells induces cellular differentiation. Science 340(6132): 622–626, 2013. PubMed: 23558173
6. Rohle D, *et al.* An inhibitor of mutant IDH1 delays growth and promotes differentiation of glioma cells. Science 340(6132): 626–630, 2013. PubMed: 23558169
7. Mondesir J, *et al.* IDH1 and IDH2 mutations as novel therapeutic targets: current perspectives. J Blood Med 7: 171–180, 2016. PubMed: 27621679